Microstructural Descriptors Characterizing Granular Deposits

Menelaos Tassopoulos and Daniel E. Rosner
High Temperature Chemical Reaction Engineering Laboratory, Chemical Engineering Dept., Yale University, New Haven, CT 06520

Quantitative results are presented on mean coordination number and coordination number distribution, contact normal distribution and fabric tensor of simulated anisotropic granular deposits with resulting solid fractions between ca. 15% for ballistic deposits and 58%, corresponding to a random loose packing. The deposits, generated by the capture of uniform size spherical particles arriving normal to a target, were simulated using a simple algorithmic model.

We focus on microstructural quantities which explicitly take into account the discrete nature of the granules comprising the deposit. Such measures are important in determining the heat transport properties of the deposits for Fourier conduction through the solid phase, as well as their mechanical and sintering properties. The variation of mean coordination number with deposit solid fraction was successfully correlated using a unit-cell model (Eq. 13). This correlation, in conjunction with entropy maximization arguments (after Nayak and Tien, 1978) has been further used to predict the coordination number distribution. The usefulness of the results reported here is illustrated by computing an upper bound to the deposit effective thermal conductivity (Jagota and Hui, 1990) and comparing it to both 'exact' simulation results (Tassopoulos and Rosner, 1991b) and experimental data (Koh, 1971).

Introduction

Packings of spheres are relevant in many fields of science and technology, including separation, chemical reaction, insulation, filtration, fouling, and material fabrication processes. Thus, the geometry and associated transport properties of packed beds and deposits derived from suspensions are of great engineering interest. Traditionally, the lowest order descriptor that has been used to characterize the deposit microstructure (in this article we refer to all particulate beds as 'deposits') is the porosity, ϵ, or, alternatively, the solid fraction, $\phi(=1-\epsilon)$. Other descriptors often used are the pore size distribution, mean coordination number and coordination number distribution and higher order n-point isotropic and anisotropic probability functions which permit the calculation of bounds to various effective transport properties of interest (see, for example, Torquato, 1987; 1991; Tassopoulos, 1991 and references therein).

In this article we present results on mean coordination number and coordination number distribution, contact normal distribution and fabric tensor (defined below) of simulated deposits consisting of uniform size particles arriving normal to the target. We focus on such microstructural quantities which explicitly take into account the discrete nature of the granules comprising the deposit, because, and as discussed in greater detail below, they are important in predicting the heat transport properties of the deposits for Fourier conduction through the solid phase (see, for example, Tassopoulos, 1991, and references therein) as well as their mechanical (see, for example, Thornton and Barnes, 1986) and sintering properties (Jagota et al., 1988). Moreover, such information is potentially useful in designing deposits with specific material or transport properties. The effect of subsequent deposit 'sintering' is also briefly addressed, using the simple grain-consolidation model (Schwartz and Banavar, 1989). The solid fraction of the unconsolidated deposits considered here ranges between ca. 15%, corresponding to the so-called ballistic deposition model, to 58%, typical of a random loose packing (Scott, 1960). Ballistic deposits (see, for example, Meakin et al., 1986) are generated by assuming that the arriving particles stick at their first contact with an already deposited particle, while the denser deposits are formed by allowing the particles to relax to positions of

lower potential energy (see, for example, Finney, 1970, and the following section).

In the following section we describe the computational model used to generate the deposits. Next, we present quantitative results on the aforementioned microstructural descriptors and compare them to available experimental data as well as theoretical predictions. Finally, we illustrate the utility of the microstructural descriptors determined in this work by evaluating a theoretical bound to the effective thermal conductivity (Jagota and Hui, 1990) with conclusions and generalizations discussed in the last section.

The Deposit Model

In this work we explore an algorithmic model to generate particulate deposits. We term 'algorithmic' all models where the rules governing interactions between individual particles and their surrounding, for example, other particles, the target surface, etc. are supplied by the user in the form of a 'recipe'. The goal of algorithmic models is, of course, to replace if possible the physics of the process by appropriate rules, that will lead to essentially the same result, say the same microstructure in a computationally more efficient way. Thus, the ballistic model mentioned in the previous section is a good example of an algorithmic model. Indeed, it is now well known that despite its evident simplicity it yields structures with geometries very similar to the ones observed in physical experiments under corresponding deposition conditions (see, for example, Vicsek, 1989). In passing we note that 'algorithmic' models are to be contrasted to 'dynamic' models. The latter explicitly incorporate the physical laws describing interactions between the particles so that the dynamical system may evolve to its desired equilibrium state (for a discussion see Tassopoulos, 1991; Konstandopoulos, 1991).

In the past, various algorithmic models have been proposed in the context of the sphere packing problem. During the 1960s and early 1970s related research advanced when it was postulated that such packings provided a model of the liquid state (Bernal, 1964; Scott, 1960; Finney, 1970). During this period several researchers developed computer codes that simulated the gentle, one at a time, gravitational deposition of spheres (Finney, 1970; Bennett, 1972; Visscher and Bolsterli, 1972; Tory et al., 1973). In the mid 1970s the emergence of the chemical vapor deposition (CVD) process as a viable technology further motivated 'ballistic' like models for amorphous solids. These molecular-level models (Henderson et al., 1974; Dirks and Leamy, 1977) successfully demonstrated, in a qualitative sense at least, some of the key features of CVD deposits. For example, it was shown that the apparent columnar microstructure that most of the resulting crystalline or amorphous thin films exhibit is due to the self-shadowing during the deposition process. However, the original models generated solids with significantly lower densities (solid fraction) than those found experimentally (see the last two references; also Meakin and Jullien, 1987) and so post-collision particle relaxation steps have been proposed that simulate either surface diffusion for CVD solids, or the effect of a weak gravitational field on the structure of deposits formed by particles sedimenting in a viscous liquid (Meakin and Jullien, 1987; Jullien and Meakin, 1987; Bennett, 1972).

Within the present framework, off-lattice algorithmic models should lead to realistic deposit microstructures in two limiting cases: Deposition of small aerosol particles with unity sticking probability and no subsequent restructuring; Deposition of larger particles that arrive at the target with nonvanishing velocity. Provided the particle kinetic energy at impact is very high and/or the adhesive forces between the particles are weak the deposits approach a possibly anisotropic (Tory et al., 1968) random loose packing configuration irrespective of the details of the particle trajectories and particle-particle interactions. Such deposits can be accurately modeled by allowing each arriving particle, after establishing contact with the existing deposit, to relax to a position of local minimum potential energy. We have used such algorithmic models to generate deposits covering the solid fraction range between about 15% for ballistic deposits generated by particles arriving at normal incidence and 58% corresponding to a random loose packing configuration. The intermediate solid fractions are obtained by appropriately adjusting the level of restructuring after the first contact with the existing deposit.

We should also point out that our deposit generation model, as summarized below, is identical to the one used by Jullien and Meakin (1987; see also Meakin and Jullien, 1987). How-

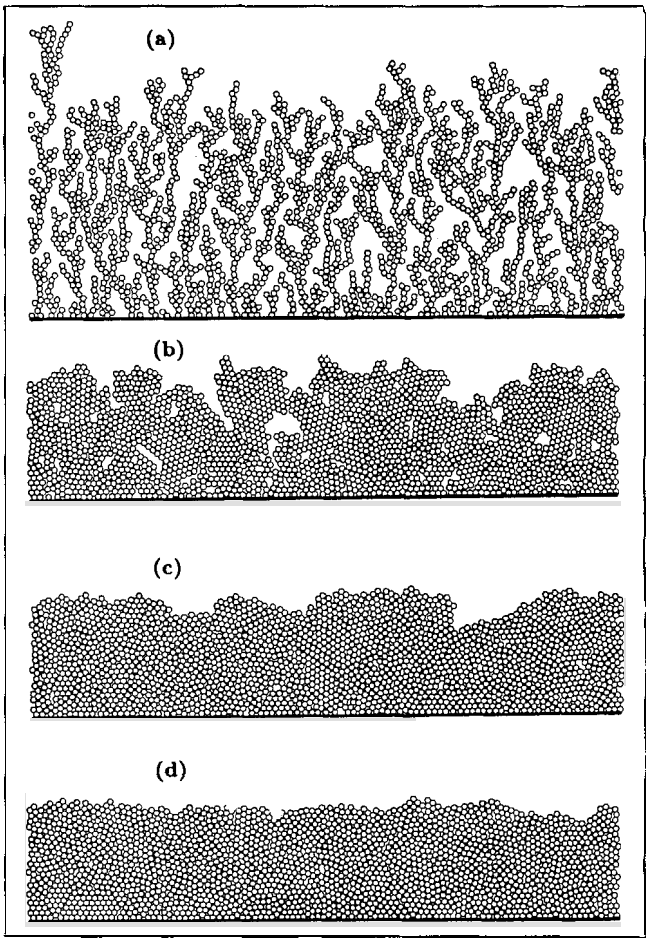

Figure 1. Typical two-dimensional deposits generated by particles following straight line trajectories, normal to the target.

a. Ballistic deposit
b. One rolling event
c. Two rolling events
d. Three rolling events

ever, while these authors have exclusively concentrated on the scaling properties of the growing interface, here we focus on the microstructural properties of the bulk of the deposit. Finally, a similar model based on the work of Tory et al. (1968; 1973) has been recently used by Reyes and Iglesia (1991) to study particle-particle contact radial profiles (descriptors similar to the radial distribution function of statistical mechanics) of random loose packings contained within cylinders. The main features of the deposition model implemented here are:

- We perform three-dimensional off-lattice simulations, with periodic boundary conditions. The incident particles, started at random positions above the existing deposit, are assumed to travel in straight lines normal to the target.
- The particles are hard, equal size, spheres.
- Already deposited particles cannot be displaced by subsequent particle arrivals: that is, we consider the so-called 'frozen' limit. For a discussion on the validity of the frozen limit assumption see Tassopoulos (1991).
- A particle that hits the target surface sticks immediately. If it hits another particle, as is likely after an initial transient, then it rolls in the direction of steepest descent. The rolling motion is continued until contact is established with another particle, in which case it continues to move towards the target while maintaining contact with both fixed particles. Each new contact between the rolling particle and another fixed particle is considered as a new 'rolling event'. If a particle while rolling reaches a position where it 'hangs' below the contacted particle then it drops vertically until it hits another particle or the target surface. Rolling is continued until the number of rolling events specified at the beginning of the simulation is completed, or the particle reaches a position of local minimum potential energy, or the original target surface is reached.

The code was optimized both in terms of memory requirements and execution speed by solving analytically for the particle linear and rolling motion and using linked lists to store the particle coordinates. Additional details and a listing of the code are provided in Tassopoulos (1991).

Results and Discussion

Deposit solid fraction

To demonstrate the dramatic effect of number of rolling events on the resulting microstructure we show in Figure 1 four off-lattice deposits generated in two dimensions (for ease of display). The first deposit (a) shown is a ballistic deposit; that is, the incoming particles stick upon first contact with already deposited ones. This deposit is characterized by rather open, microcolumnar structures. The other three were generated by particles that undergo, respectively, one rolling event (deposit b), two (deposit c) and three (deposit d) rolling events. The effect of the rolling on the deposit microstructure is apparent, especially when compared to the pure ballistic deposit (a). Note further, that the difference in the final solid fraction between deposits (c) and (d) is very small, an effect we also observed in the full three-dimensional (3D) simulations.

Our quantitative results are based on 3D off-lattice deposits generated on targets 60×60 particle diameter wide and represent averages of five independent realizations. In all simulations the length scale is set by the particle diameter. We have measured the deposit solid fraction or, alternatively, the porosity, $\epsilon(=1-\phi)$, using two independent techniques. Since ϕ can be interpreted as the geometric probability for a random point to belong to the solid phase, it can be obtained by throwing N random points in the deposit, say at positions $\mathbf{r}_i$, and determining whether they belong to the solid phase. Formally,

$$\phi=\lim_{N\to\infty}\frac{1}{N}\sum_{i=1}^{N}I_s(\mathbf{r}_i) \tag{1}$$

where $I_s(\mathbf{r})$ an indicator function equal to unity if $\mathbf{r}$ is in the solid phase and zero otherwise. We found that as long as N was greater or equal to 10^5 we obtained very reproducible results that were independent of N. Since it is well known that the generated deposits are homogeneous only in the region away from the underlying target and the growing outer surface (Jullien and Meakin, 1987; Meakin and Jullien, 1987; Family and Vicsek, 1987), all our results are based on porous samples at least 25 particle diameters away from the deposit edges. For macroscopically homogeneous deposits, the solid fraction is also related to the deposit mean height. In a manner analogous to on-lattice simulations (Family and Vicsek, 1985) we define the deposit mean height by:

$$\bar{h}\equiv\frac{1}{(L/d)^2}\sum_{i,j}h_{i,j} \tag{2}$$

where L the actual target width, d the discretization length, and h_{ij} the local height at the ijth position obtained by a ray-tracing technique. A value for d of $\frac{1}{4}$ provided an acceptable compromise between accuracy and execution speed, with the solid fractions predicted by Eqs. 1 and 3 agreeing to within 1.5%. Given $\bar{h}$, the mean solid fraction was determined from

$$\phi=\frac{V_{\text{solid}}}{L^2\times\bar{h}} \tag{3}$$

where V_{solid} the total volume of the particles present in the deposit. The effect of number of rolling events on final deposit solid fraction is shown in Figure 2 (see also Table 1, where we have compiled several microstructural descriptors of interest). The dependence of ϕ as computed by Eq. 1 on number of rolling events, shown in Figure 2 and Table 1, is identical to the one predicted by Jullien and Meakin (1987) providing an independent confirmation of our deposit generation code. Finally, and as already pointed out by Jullien and Meakin (1987) the maximum solid fraction value of 0.58 obtained when allowing the particles to roll to the position of minimum potential energy is in good agreement with the experimental value of 0.57 obtained in a sedimentation experiment of noncolloidal spherical glass beads in water (Bacri et al., 1986), performed gently enough so that multiparticle restructuring events were absent.

Mean coordination number

The solid fraction, ϕ, is the lowest order microstructural descriptor. An additional physically relevant characterization of the deposit microstructure is provided by the mean coordination number, $\bar{Z}$, which for a macroscopically homogeneous deposit is related to ϕ by

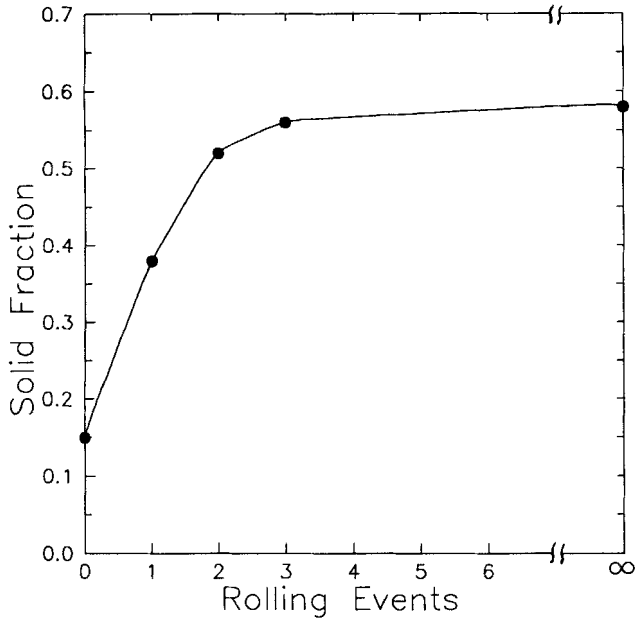

Figure 2. Effect of rolling events on deposit solid fraction.

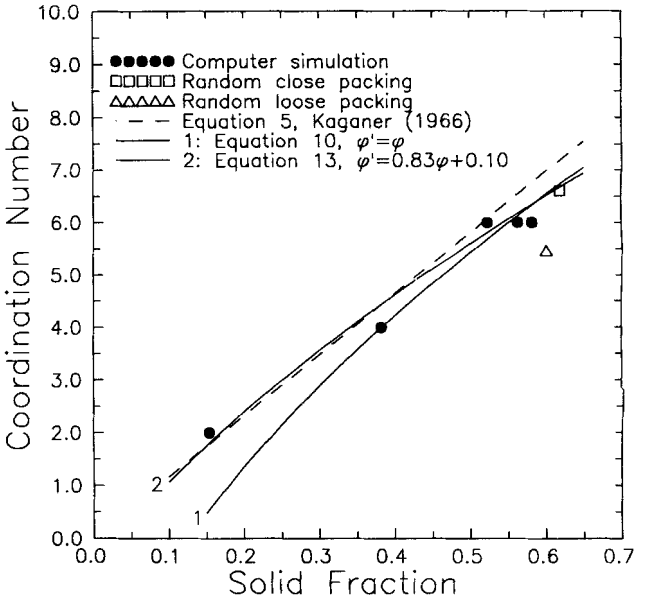

Figure 3. Variation of mean coordination number, $\bar{Z}$, with deposit solid fraction, ϕ.

The dashed line corresponds to an empirical correlation reported by Kaganer (1966; Eq. 5); the solid lines to Eqs. 10 and 13.

$$\bar{Z}=\frac{2\bar{M}}{\phi}\cdot V_p=\frac{8\pi R_p^3\bar{M}}{3\phi} \tag{4}$$

where $\bar{M}$ is the number of particle contacts per unit volume, V_p the volume of a single particle, and R_p its radius. In Table 1 we give the deposit solid fraction, mean coordination number and its standard deviation, σ_Z, as a function of number of post-arrival rolling events. σ_Z is defined here in terms of expectation values by $\{E[Z^2]-(E[Z])^2\}^{1/2}$. In Figure 3 we plot mean coordination number, $\bar{Z}$, vs. ϕ for the deposits considered here. The filled circles are the data obtained in the current work, while the empty symbols correspond to mean coordination numbers of real random-dense and random-loose packings, obtained by Bernal and Mason (1960) using a dye technique. The dashed line on the same figure depicts an empirical fit reported by Kaganer (1966). Kaganer gives the following linear relationship between deposit solid fraction and mean coordination number:

$$\bar{Z}=11.6\phi \tag{5}$$

which is also in quite good agreement with our data.

There is clearly no theoretical or experimental evidence (see, for example, Figures 3 and 5) to suggest that there is a one-to-one correspondence between deposit solid fraction and mean coordination number. On the other hand moments of the coordination number and contact normal *distributions* are very important in determining the deposit strength, heat transport properties, sintering characteristics, and condensible vapor uptake rate. Thus, it is instructive to consider the following simple unit-cell model (see, for example, Ouchiyama and Tanaka, 1981) for predicting a relationship between $\bar{Z}$ and ϕ, especially since such unit-cell models are also useful in estimating effective properties of interest (Tassopoulos and Rosner, 1991b).

Table 1. Effect of Number of "Rolling Events" on Deposit Solid Fraction, Mean Coordination Number, and Coordination Number Standard Deviation

Rolling Events	ϕ	$\bar{Z}$	σ_Z
0	0.15	1.99	0.73
1	0.38	3.99	1.19
2	0.52	5.99	1.33
3	0.56	5.99	1.08
Min. Potential	0.58	6.00	0.98

Consider a test sphere, of radius equal to one particle diameter, and concentric with some typical particle, O_1 (see Figure 4). Let the average solid fraction within the test sphere be ϕ'. For relatively dense deposits, we expect that $\phi'\to\phi$. On the other hand, for more open deposits formed without significant post-collisional restructuring the 'connectedness' constraint, namely, that every particle must be in contact with at least another particle, results to a 'local' solid fraction ϕ' greater than the 'global' average value, ϕ. In general, we may write:

$$\phi'=\frac{V_{\text{solid}}}{V_{\text{sphere}}} \tag{6}$$

where $V_{\text{sphere}}=4\pi(2R_p)^3/3$ and V_{solid} the total solid volume within the test sphere. V_{solid} will receive contributions from the center particle, O_1, from particles in direct contact with the center particle, denoted in Figure 4 as O_2, from particles O_3 that are in contact with particles O_2 and penetrate the test sphere, etc. Thus, if $\bar{Z}$ is the mean coordination number:

$$V_{\text{solid}}\simeq\frac{4\pi R_p^3}{3}+\bar{Z}\cdot\Delta V_2+\frac{1}{2}(\bar{Z})^2\cdot\overline{\Delta V_3}+\ldots \tag{7}$$

where ΔV_2, and ΔV_3 are the volumes of O_2 and O_3 belonging

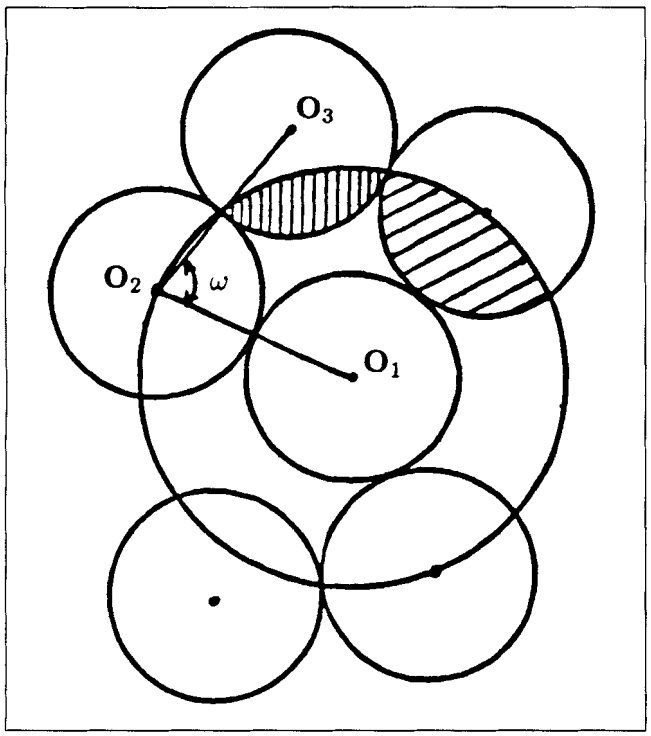

Figure 4. Geometry assumed for the derivation of the mean coordination number correlation, Eq. 13.

to the test sphere (hatched regions in Figure 4). The 1/2 factor in front of $\overline{Z}^2$ has been included to avoid double counting second order contributions to the solid volume.

In writing Eq. 7 we neglected terms that represent particles contributing to V_{solid} but not in direct contact with the center particle or its neighbors as well as higher order contributions. The former may be important only for intermediate solid fraction deposits ($\phi \simeq 0.30$) while the latter are always negligible. It is straightforward to show that $\Delta V_2 = (13/24)\pi R_p^3$. ΔV_3 depends on the angle, ω, formed between O_2O_1 and O_2O_3. We find

$$\Delta V_3(y) = \frac{(-3+4y)^2(-3+24y+16y^2)}{48y}, \quad \frac{1}{2} \le y \le \frac{3}{4} \tag{8}$$

where $y \equiv \sin(\omega/2)$. Assuming next that all values of ω are equally probable, that is, neglecting the anisotropy associated with the contact normal distribution, we estimate

$$\overline{\Delta V_3} = \left[\int_{\pi/3}^{\pi} \sin\omega d\omega\right]^{-1} \cdot \int_{\pi/3}^{\omega_{max}} \Delta V_3(\omega) d\omega = \frac{13}{180}\pi R_p^3 \tag{9}$$

where $\omega_{max} = 2\sin^{-1}(3/4)$. Finally, combining Eqs. 6, 7 and 9 and solving for $\overline{Z}$ we obtain

$$\overline{Z}(\phi') = \frac{-195 + [38{,}025 - 52(480 - 3{,}840\phi')]^{1/2}}{26} \tag{10}$$

The solid line 1 of Figure 3 corresponds to equation 10 with $\phi = \phi'$. As already rationalized, this theoretical expression agrees with the simulation data for deposits with mean solid fraction greater than about ca. 35%. In order to predict the $\overline{Z}$ values corresponding to more open deposits ($\phi < 0.35$) we must incorporate into the model the connectivity constraint. This can be achieved as follows. Employing the same argument used to derive Eq. 7 and neglecting second-order contributions, not a bad assumption in the low ϕ limit, we find that

$$\phi' \simeq \frac{\frac{4}{3}\pi R_p^3 + \overline{Z}\cdot\frac{13}{24}\pi R_p^3}{\frac{4}{3}\pi(2R_p)^3} \tag{11}$$

For $\overline{Z} = 2$ Eq. 11 predicts $\phi' \simeq 0.23$, while the corresponding average solid fraction, Table 1, is 0.15. Using this observation and further assuming a linear relationship between ϕ and ϕ' yields

$$\phi' \simeq 0.83\phi + 0.10 \tag{12}$$

where $\phi'(\phi = 0.60) = 0.60$. Substituting Eq. 12 into Eq. 11 gives

$$\overline{Z}(\phi) = \frac{-195 + [38{,}025 - 52(96 - 3{,}187\phi)]^{1/2}}{26} \tag{13}$$

This correlation, also plotted on Figure 3 (line 2), predicts the simulation data successfully over the whole solid fraction range considered.

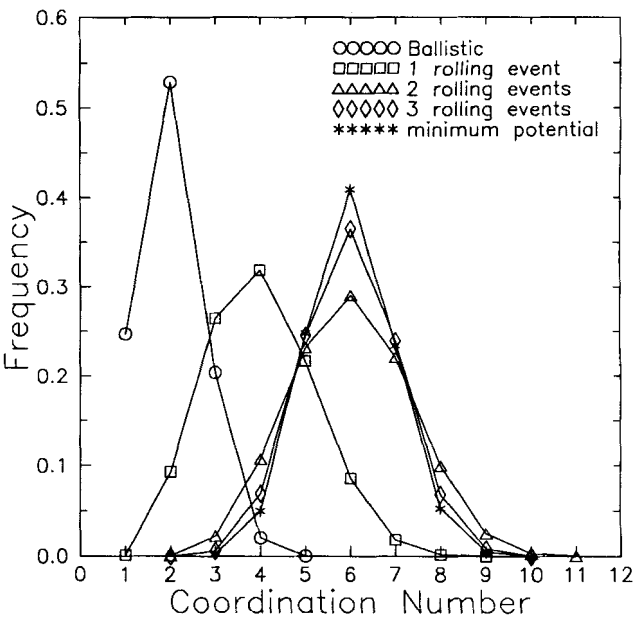

Figure 5. Normalized histogram of the coordination number distribution in a ballistic deposit without post-arrival restructuring, and denser deposits.

Coordination number distribution

In Figure 5 we plot a normalized histogram (frequency distribution) of the coordination number distribution for a ballistic deposit without restructuring as well as denser deposits. As expected, with increasing solid fraction the distribution

Table 2. Coordination Number Distribution

Coordination	Ballistic	1 Rolling	2 Rolling	3 Rolling	Min. Potential
1	2.47E-1	1.30E-3	—	—	—
2	5.28E-1	9.29E-2	7.55E-4	1.23E-5	—
3	2.04E-1	2.64E-1	2.21E-2	5.98E-3	2.42E-3
4	2.03E-2	3.19E-1	1.07E-1	6.90E-2	4.98E-2
5	3.15E-4	2.17E-1	2.31E-1	2.45E-1	2.47E-1
6	—	8.58E-2	2.90E-1	3.65E-1	4.09E-1
7	—	1.81E-2	2.21E-1	2.39E-1	2.34E-1
8	—	2.05E-3	9.95E-2	6.82E-2	5.28E-2
9	—	7.24E-5	2.50E-2	7.88E-3	4.73E-3
10	—	—	3.17E-3	2.83E-4	8.54E-5
11	—	—	2.91E-4	—	—

shifts towards larger coordination numbers. Moreover, as the number of rolling events increases, and hence the system has more freedom to reach its own equilibrium state, the spread of the coordination number distribution decreases. The distributions on Figure 5 are also tabulated in Table 2.

Next we briefly consider ways to predict the coordination number distribution from first principles. To our knowledge Beresford (1969) was the first to derive a set of statistical equations governing the coordination number distribution, as a function of deposit solid fraction and mean coordination number. Given that a test particle had z contacts and considering the probability of a new contact being made, in the steady-state limit he predicted a binomial type distribution for the frequency of z contacts:

$$p_z = \left(\frac{\bar{Z}-m}{C-\bar{Z}}\right)^{z-m}\left(\frac{C-\bar{Z}}{C-m}\right)^{C-m}\frac{(C-m)!}{(z-m)!(C-z)!} \qquad (14)$$

where $C = 14.93\phi$ and m is the minimum permissible number of contacts for deposit stability, taken here as 3. In Figure 6a, we compare Beresford's prediction (solid line) to our computer simulation results for a deposit corresponding to 2 rolling events and in Figure 6b for a deposit generated by particles rolling to the position of minimum potential energy. Note that the agreement in both cases is quite good. For completeness we also show in Figure 6b an experimentally obtained coordination number distribution (filled circles) reported by Bernal and Mason (1960) for a random loose packing with $\phi = 0.60$.

Another approach to predict the coordination number distribution (or any distribution for that matter) is based on entropy maximization arguments. This approach has been used quite successfully to analyze various physical phenomena including the particle size distribution associated with coagulation-aged aerosols and sprays (Rosen, 1984; Li and Tankin, 1987), cluster size distribution of colloidal particles in stirred suspensions (Cohen, 1990), capture probability of colloidal particles (Cohen, 1989), and coordination number distribution in packed beds (Nayak and Tien, 1978). The analysis presented here follows Nayak and Tien (1978; see also Eyring et al., 1982) with the difference that we used a different constitutive relation to link local coordination number and local solid fraction, and have added an extra constraint on the mean coordination number in order to obtain better agreement between the simulation data and the theoretical prediction.

Let the coordination number be distributed over a number of microstates. Clearly, for a packed bed consisting of single-size spherical particles (present case), the coordination number can vary between 1 and 12, while for a sufficiently polydispersed population, it may be continuously distributed. With each microstate z let us associate a probability of occurrence, $p_z \equiv N_z/N_p$, where N_z the number of particles with coordination number z and N_p the total number of particles in the deposit. An obvious constraint on the p_z is that they must be non-negative and furthermore

$$\sum_{z=1}^{12} p_z = 1 \qquad (15)$$

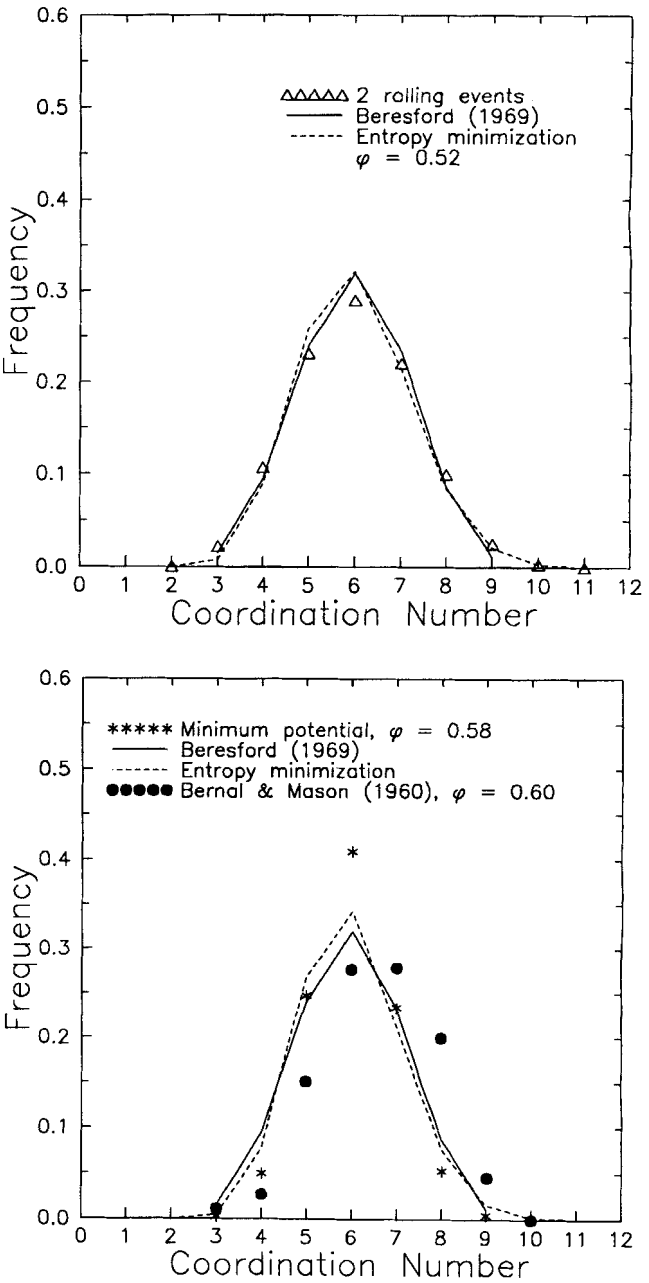

Figure 6. Actual coordination number vs. theoretical predictions based on the binomial distribution.

Solid line (Beresford, 1969); dashed lines (entropy maximization arguments). (a) Deposit solid fraction, $\phi = 0.52$; (b) $\phi = 0.58$.

Each microstate, that is, each coordination number, z, corresponds to a local solid fraction ϕ_z. The relationship between local coordination number and local solid fraction can be based on any appropriate constitutive relation, such as Eq. 5 (the one used by Nayak and Tien, 1978) or Eq. 13 (see also Tassopoulos, 1991). In the following analysis we use Eq. 13 to establish this connection. Having obtained a relationship between z and ϕ_z, the requirement that the total deposit volume be conserved can be expressed as (see, Nayak and Tien, 1978):

$$\sum_{z=1}^{12} p_z \frac{1}{\phi_z} = \frac{1}{\phi} \tag{16}$$

Initially we tried to use only Constraints 15 and 16 (as done by Nayak and Tien) but the resulting theoretical distributions had means consistently higher than the actual ones. To obtain better agreement, we imposed an extra constraint by fixing the mean coordination number. Note that, given the deposit mean solid fraction, $\overline{Z}$ can be readily obtained from Eq. 13. This final constraint states that

$$\sum_{z=1}^{12} p_z z = \overline{Z} \tag{17}$$

The principle of maximum entropy requires that we determine the distribution which avoids any bias, that is, the most probable one, while satisfying the available constraints, Eqs. 15, 16 and 17. From statistical mechanics we know that the total number of ways of achieving a macroscopic state of the system such that N_z particles have coordination number z is (see, for example, Eyring et al., 1982)

$$W = N_p! \prod_{z=1}^{12} \frac{g_z^{N_z}}{N_z!} \tag{18}$$

where g_z is the degeneracy associated with each microstate. The degeneracy of any state is simply the number of different ways z levels can be distributed over 12 levels (the largest permissible coordination number for uniform size spheres) independently of order (Nayak and Tien, 1978). Thus

$$g_z = \frac{12!}{z!(12-z)!} \tag{19}$$

The most probable distribution corresponds to p_z values which maximize W or, equivalently, $\ln W$ subject to the constraints given by Eqs. 15-17. Using the theory of Lagrange multipliers we find

$$p_z = \frac{N_z}{N_p} = \frac{g_z \exp[\lambda_2/\phi_z + \lambda_3 z]}{\sum_{z=1}^{12} g_z \exp[\lambda_2/\phi_z + \lambda_3 z]} \tag{20}$$

where λ_2 and λ_3 are the second and third Lagrange multipliers and the denominator is the partition function of statistical mechanics. The first Lagrange multiplier was eliminated with the help of Eq. 15. Substituting the expression for p_z in Eq. 18 and maximizing with respect to λ_2 and λ_3 we end up with a set of two nonlinear algebraic equations:

$$\sum_{i=1}^{12} \left(\frac{1}{\phi} - \frac{1}{\phi_z}\right) g_z \exp[\lambda_2/\phi_z + \lambda_3 z] = 0 \tag{21a}$$

and

$$\sum_{i=1}^{12} (\phi - \phi_z) g_z \exp[\lambda_2/\phi_z + \lambda_3 z] = 0 \tag{21b}$$

which were solved using a Newton-Raphson technique. The theoretical predictions of the coordination number distribution based on the information entropy are also shown in Figures 6a and 6b (dashed lines). The agreement between theory and simulation data is again quite good.

Contact normal distribution and fabric tensor

It has been long realized that particle deposition from the gas phase leads to anisotropic structures, for example, Figure 1. Furthermore, the local anisotropy, in conjunction with the closeness of the packing of the individual particles, will strongly influence both the transport and mechanical properties of the deposit. We have already indicated that the solid fraction, ϕ, and the mean coordination number, $\overline{Z}$, are useful scalar quantities characterizing the compactness of the deposit. On the other hand a more complete description of the structural anisotropy clearly requires a tensorial approach. In this section we consider the anisotropy associated with the distribution of the contact normals, $\mathbf{n}$, (Onat and Leckie, 1988; Seibert, 1988; Thornton and Barnes, 1986). A random distribution is associated with a macroscopically isotropic structure, while nonuniformities in the distribution indicate anisotropy. Although a complete description of an arbitrary anisotropic microstructure may require a representation in terms of an infinite series of increasing-order tensors (see e.g., Onat and Leckie, 1988),

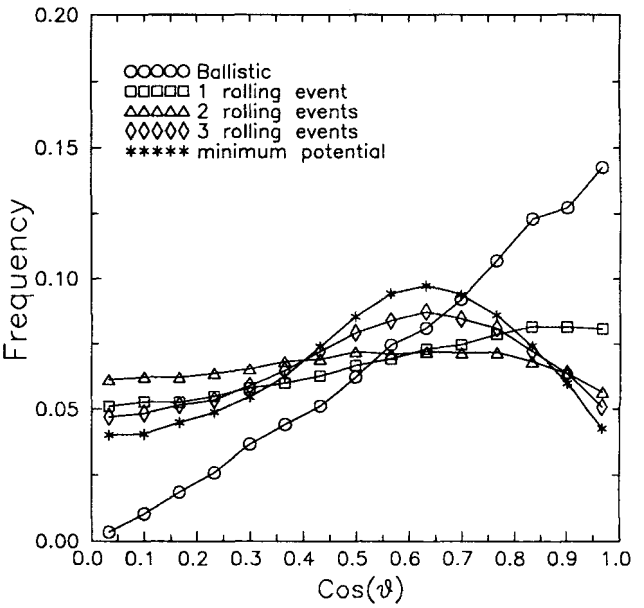

Figure 7. Probability density distribution of the cosine of the angle formed between the normal to the target and the line of centers between particles in contact.

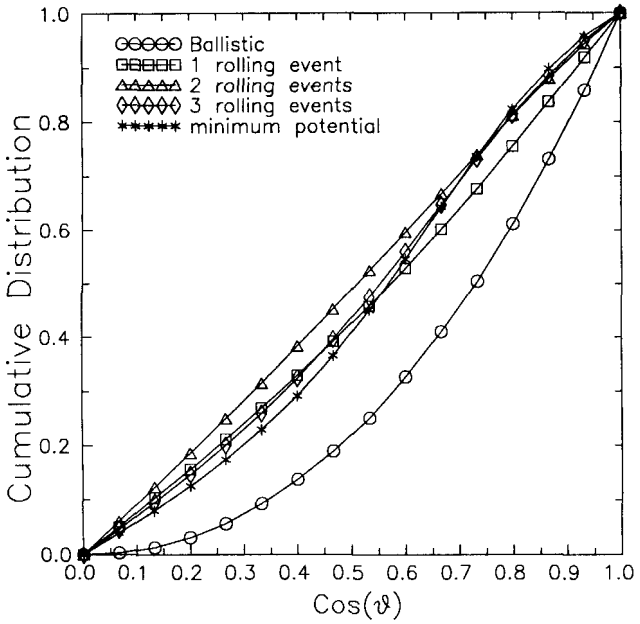

Figure 8. Cumulative distributions of the cosine of the angle formed between the normal to the target *and the line of centers between particles in* contact.

the principal directions of anisotropy of deposits formed by discrete particles are usually defined to be the eigenvectors of the fabric tensor. The fabric tensor, $\mathfrak{F}$, is a symmetric second rank tensor which for an assembly of monodispersed spherical particles can be written (Oda et al., 1982; Satake, 1985):

$$\mathfrak{F}=\frac{3\phi\overline{Z}}{4\pi R_p^2}\langle \mathbf{nn}\rangle \tag{22}$$

where $\mathbf{n}$ denotes the contact normal vector and the angular brackets denote an ensemble average. Note that the fabric tensor incorporates information on both the closeness of the packing and the anisotropy. The distribution of θ, the angle formed between the z-axis and the contact normal, is of interest as well, especially for deposits possessing azimuthal symmetry; this is, deposits generated by particles arriving normal to the target. In Figure 7 we plot the probability density distribution, $f(x)$, of $x\equiv\cos\theta$ for various deposits generated at normal incidence, and in Figure 8 we show the corresponding cumulative distributions, $F(x)$. In Table 3 we provide polynomial least square fits to the cumulative distributions of Figure 8. Finally, in Table 4 we have tabulated the eigenvalues of the fabric tensor for the various deposits considered here.

Illustrative Application

Although it is clearly beyond the scope of the present paper to illustrate all the physical or engineering problems which involve the microstructural quantities determined here, it is instructive to briefly consider a particular example. Thus we evaluate an upper bound to the effective thermal conductivity tensor of packed beds, reported by Jagota and Hui (1990; see also Tassopoulos and Rosner, 1991b). Jagota and Hui used a volume-average approach in the spirit of Batchelor and O'Brien

Table 3. Least Square Fit to the Cumulative Distribution Function of the Angle Formed Between the Normal to the Target Surface and the Contact Normal

$F(x)=\alpha+\beta x+\gamma x^2+\delta x^3+\epsilon x^4$, where $x=\cos\theta$

Rolling Events	α	β	γ	δ	ϵ
0	—	−0.0135	0.799	0.215	—
1	−0.0050	1.135	−0.123	—	—
2	−0.0028	0.988	0.0209	—	—
3	−0.0046	0.842	0.464	−0.305	—
Min. Potential	—	0.656	−0.749	3.231	−2.142

Table 4. Eigenvalues of the Fabric Tensor

Rolling Events	$\frac{3\phi\overline{Z}}{4\pi}$	n_{11}*	n_{22}	n_{33}
0	0.072	0.235	0.241	0.524
1	0.363	0.308	0.311	0.381
2	0.745	0.333	0.333	0.334
3	0.802	0.323	0.324	0.353
Min. Potential	0.831	0.320	0.321	0.359

*11, 22 directions parallel to the target; 33 normal to the target.

(1977) in conjunction with a mean temperature field assumption to derive the following anisotropic upper bound to the true effective thermal conductivity, $\mathbf{K}^*$, of the bed:

$$\mathbf{K}^*\le\frac{3}{\pi R_p}\phi\overline{Z}\rho\langle \mathbf{nn}\rangle k_1 \tag{23}$$

where ρ the radius of the particle contact area, assumed here constant, and k_1 the intrinsic thermal conductivity of the par-

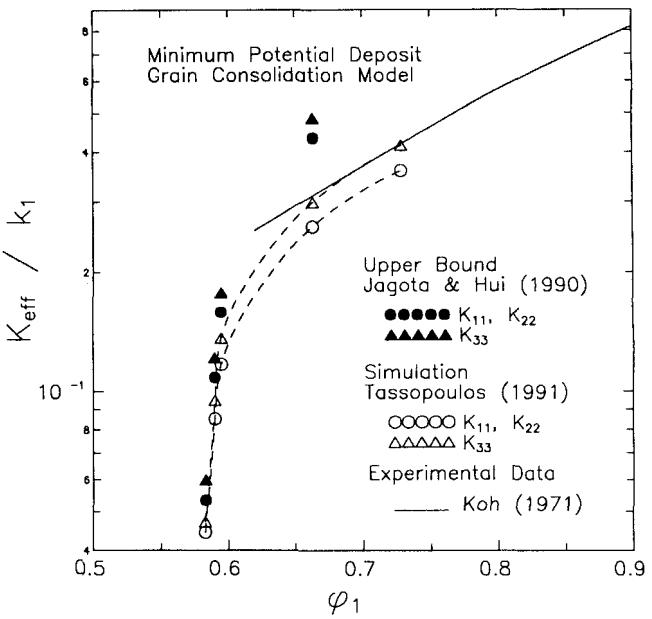

Figure 9. Anisotropic effective thermal conductivity of consolidated deposits possessing azimuthal symmetry.

Comparison of an upper bound (filled symbols), "exact" simulation results (empty symbols) and experimental data (solid line).

ticulate phase. Using the data provided in Tables 1 and 4 we computed the upper bound to k_{eff} for heat conduction parallel to the target surface (note that the azimuthal symmetry of the deposits results in $K_{11} = K_{22}$; filled circles in Figure 9) and normal to the target (K_{33}; filled triangles in Figure 9). Here, we considered deposits generated by particles rolling to positions of minimum potential energy and at different levels of consolidation. Compaction of the deposits was achieved using the so-called grain consolidation model (see, for example, Schwartz and Banavar, 1989). According to this model the radii of all particles are increased by a fixed amount, so that particles originally in point contact interpenetrate. Despite its simplicity this model has been used quite extensively and successfully to study the effective void diffusivity and permeability of beds of consolidated particles due to sintering or growth (see, for example, Schwartz and Banavar, 1989; Reyes and Iglesia, 1991). Finally, we should point out that when the particle radii of the original unconsolidated particles are increased significantly (say above 25%) many new contacts are formed and so the data of Tables 1-4 must be corrected (for related properties of consolidated deposits see Tassopoulos, 1991). However, for the relatively small consolidation levels considered in this work, Tables 1-4 remain valid.

The upper bound of Jagota and Hui can be further compared to simulation data on $\mathbf{K}_{eff}$ obtained by our group (Tassopoulos, 1991). We have used a Brownian diffusion simulation technique (see, for example, Hong et al., 1986; Kim and Torquato, 1991) to determine 'exactly' the deposit effective thermal conductivity tensor from the slope of mean square displacement vs. time of heat tracers diffusing through the porous medium in the limit of large time. Details on the computational method and extensive results are expected to be reported in future publications (see, for example, Tassopoulos and Rosner, 1991b). The anisotropic simulation data are denoted in Figure 9 by the empty symbols, the circles corresponding to the effective thermal conductivity in directions parallel to the target, K_{11}, and the empty triangles to K_{33}. Note that indeed the 'exact' values are always below the corresponding upper bounds (for the densest deposit with $\phi = 0.73$ we do not indicate the upper bounds because the formation of new contacts is significant so that Tables 1 and 4 are not valid). Moreover the bounds are quite tight, especially in the low consolidation limit (small ρ). Finally, on the same figure we show the experimental data of Koh (1971; solid line) who measured the effective thermal conductivity of consolidated stainless steel particles. His data are in very good agreement with our simulation results, further supporting the grain consolidation model as a simple way of modelling sintered packed beds.

Conclusions and Generalizations

In this communication we presented quantitative results on the coordination number distribution, contact normal distribution and fabric tensor of particulate deposits. For computational efficiency, the deposits were generated using an algorithmic model. Despite its simplicity, this model predicts microstructures which in certain limits are very 'similar' (as, for example, determined by the radial distribution function) to real-life deposits (see, for example, Zallen, 1979) or to deposits generated with more realistic dynamic models (Konstandopoulos and Tassopoulos, 1990; Tassopoulos, 1991). Furthermore, since quite often we are only interested in effective material or transport properties (which involve volume integrals of these descriptors) use of the data presented here should be justifiable, even when the finer details of the deposit of interest and the corresponding deposit analyzed here are not exactly the same (see, previous section and, especially, Figure 9; also Tassopoulos, 1991).

To facilitate the use of our results by the engineering community, we have presented them in tabular format and further provided theoretical and/or empirical fits. Thus, using a unit-cell approach (see, for example, Ouchiyama and Tanaka, 1981) we were able to successfully predict the variation of mean coordination number with deposit solid fraction, Eq. 13. Similarly, following Nayak and Tien (1978), we have used entropy maximization arguments, in conjunction with the mean coordination number correlation proposed here (Eq. 13), to predict the coordination number distribution of the various deposits. The agreement between theory and simulation was again good.

Finally, we conclude by providing a list of several engineering problems that require at least some knowledge of the geometric descriptors determined here: Mechanics and strength of granular media (see, for example, Oda et al., 1982; Satake, 1985; Thornton and Barnes, 1986), size distribution of particles during granulation (Ouchiyama and Tanaka, 1981), sintering properties of packed beds (Jagota et al., 1988), Knudsen diffusion of vapors (Tassopoulos and Rosner, 1991a), sticking probabilities of particles impacting on beds of already deposited particles (Konstandopoulos, 1991; Rosner, et al., 1991) and deposit heat transport properties, primarily for Fourier conduction through the solid phase (see, for example, Batchelor and O'Brien, 1977, Nayak and Tien, 1978; Jagota and Hui, 1990; Tassopoulos, 1991; Tassopoulos and Rosner, 1991b). As an illustration (see, previous section) we evaluated an upper bound to the effective thermal conductivity tensor (Jagota and Hui, 1990) and compared it to corresponding 'exact' results obtained by Brownian diffusion simulations (Tassopoulos, 1991), as well as experimental data (Koh, 1971). Future work on the algorithmic deposits considered in this paper will include predictions of the response of the deposit surface to impulsive heating of the substrate/deposit interface, with potential application to new nondestructive diagnostic techniques based on digital thermography.

Acknowledgment

This research was supported, in part, by the U.S. Department of Energy-Pittsburgh Energy Technology Center via Grant DE-FG22-90 PC 90099, and the 1990 Industrial Affiliates of the Yale High Temperature Chemical Reaction Engineering (HTCRE) Laboratory: DuPont, Shell Corp. and Union Carbide. The authors would also like to thank Dr. A. G. Konstandopoulos and Professors S. Torquato and J. A. O'Brien for their comments and helpful discussions throughout this work.

Notation

d = discretization length (Eq. 2)
$E[\ ]$ = expected value
$\mathfrak{F}$ = fabric tensor
g_z = degeneracy of z microstate
$\bar{h}$ = deposit mean height
I_s = indicator function
k_1 = intrinsic thermal conductivity of solid phase
$\mathbf{K}^*$ = true deposit effective thermal conductivity tensor
L = target width
m = minimum number of contacts for deposit stability

$\overline{M}$ = average number of contacts per unit volume
$\mathbf{n}$ = contact normal
N = number of random test-points used to determine ϕ
N_p = total number of particles in deposit
N_z = number of particles with coordination number z
p_z = probability of having local coordination number z
$\mathbf{r}$ = position vector
R_p = particle radius
V = volume
V_p = particle volume
W = number of different ways of distributing N_p particles over 12 microstates (coordination numbers)
x = $\cos\theta$
y = $\sin(\omega/2)$
$\underline{z}$ = local coordination number
$\overline{Z}$ = mean coordination number
$\langle\ \rangle$ = ensemble average

Greek letters

ΔV = common volume (Eq. 7)
ϵ = porosity
θ = angle formed between contact normal and z-axis
λ_i = Lagrange multiplier, $i = 1, 3$
ρ = radius of contact area
σ_Z = spread of coordination number distribution
ϕ = bulk solid fraction
ϕ' = local solid fraction (Eq. 6)
ϕ_z = solid fraction associated with coordination z
ω = angle formed between O_2O_1 and O_2O_3 (Figure 4)

Literature Cited

Bacri, J. C., C. Frénois, M. Hoyos, R. Perzynski, N. Rakotomalala, and D. Salin, "Acoustic Study of Suspension Sedimentation," *Europhys. Lett.*, **2**(2), 123 (1986).

Batchelor, G. K., and R. W. O'Brien, "Thermal or Electrical Conduction through a Granular Material," *Proc. R. Soc. Lond.*, **A 355**, 313 (1977).

Bennett, C. H., "Serially Deposited Amorphous Aggregates of Hard Spheres," *J. Appl. Phys*, **43**(6), 2727 (1972).

Beresford, R. H., "Statistical Geometry of Random Heaps of Equal Spheres," *Nature*, **224**, 550 (1969).

Bernal, J. D., "The Structure of Liquids," *Proc. R. Soc.*, **A 280**, 299 (1964).

Bernal, J. D., and J. Mason, "Packing of Spheres," *Nature*, **188**, 908 (1960).

Cohen, R. D., "The Probability of Capture and its Impact on Floc Structure," *J. Chem. Soc. Faraday Trans.*, **85**(9), 1487 (1989).

Cohen, R. D., "Steady-State Cluster Size Distribution in Stirred Suspensions," *J. Chem. Soc. Faraday Trans.*, **86**(12), 2133 (1990).

Dirks, A. G., and H. J. Leamy, "Columnar Microstructure in Vapor-Deposited Thin Films," *Thin Solid Films*, **47**, 219 (1977).

Eyring, H., D. Henderson, B. J. Stover, and E. M. Eyring, *Statistical Mechanics and Dynamics*, Wiley, New York (1982).

Family, F., and T. Vicsek, "Scaling of the Active Zone in the Eden Process on Percolation Networks and the Ballistic Deposition Model," *J. Phys. A:Math Gen.*, **18**, L75 (1985).

Finney, J. L., "Random Packings and the Structure of Simple Liquids I. The Geometry of Random Close Packing," *Proc. R. Soc. Lond.*, **A 319**, 479 (1970).

Henderson, D., M. H. Brodsky, and P. Chaudhari, "Simulation of Structural Anisotropy and Void Formation in Amorphous Thin Films," *Applied Phys. Letters*, **25**(11), 641 (1974).

Hong, D. C., H. E. Stanley, A. Coniglio, and A. Bunde, "Random Walk Approach to the Two-Component Random-Conductor Mixture: Perturbing Away from the Perfect Random Resistor Network and Superconducting-Network Limits," *Phys. Rev.*, **B 33**(7), 4564 (1986).

Jagota, A., P. R. Dawson, and J. T. Jenkins, "An Anisotropic Continuum Model for the Sintering and Compaction of Powder Packings," *Mechanics of Materials*, **11**, 357 (1988).

Jagota, A., and C. Y. Hui, "The Effective Thermal Conductivity of a Packing of Spheres," Trans. ASME, *J. Applied Mech.*, **57**, 789 (1990).

Jullien, R., and P. Meakin, "Simple Three-Dimensional Models for Ballistic Deposition with Restructuring," *Europhys. Lett.*, **4**(12), 1385 (1987).

Kaganer, M. G., "Contact Heat Transfer in Granular Material under Vacuum," *J. Engineering Phys.*, **11**(1), 19 (1966).

Koh, J. C. Y., in J. S. Agapiou, and M. F. DeVries, "An Experimental Determination of the Thermal Conductivity of Stainless Steel Powder Metallurgy Material," *J. Heat Transfer*, ASME Trans., **111**, 281 (1989).

Kim, I. C., and S. Torquato, "Determination of the Effective Conductivity of Heterogeneous Media by Brownian Motion Simulation," *J. Appl. Phys.*, **68**, 3892 (1991).

Konstandopoulos, G. K., *Effect of Particle Inertia on Aerosol Transport and Deposit Growth Dynamics*, PhD Thesis, Yale University (1991).

Konstandopoulos, A. G., and M. Tassopoulos, "Simulation of Particle Impaction: Sticking Probability and Microstructure Evolution in the 'Frozen' Deposit Limit," *AAAR Meeting*, Philadelphia, PA, paper 6E.6 (1990); Manuscript prepared for submission to *J. Colloid Interf. Sci.* (1990).

Li, X., and R. S. Tankin, "Droplet Size Distribution: A Derivation of a Nukiyama-Tanasawa Type Distribution Function," *Comb. Sci. Tech.*, **56**, 65 (1987).

Meakin, P., and R. Jullien, "Restructuring Effects in the Rain Model for Random Deposition," *J. Physique*, **48**, 1651 (1987).

Meakin, P., P. Ramanlal, L. M. Sander, and R. C. Ball, "Ballistic Deposition on Surfaces," *Phys. Rev.*, **A 34**(6), 5091 (1986).

Nayak, A. L., and C. L. Tien, "A Statistical Thermodynamic Theory for Coordination Number Distribution and Effective Thermal Conductivity of Random Packed Beds," *Int. J. Heat Mass Transfer*, **21**, 669 (1978).

Oda, M., S. Nemat-Masser, and M. M. Mehrabadi, "A Statistical Study of Fabric in a Random Assembly of Spherical Granules," *Int. J. Anal. Methods in Geomech.*, **6**, 77 (1982).

Onat, E. T., and F. A. Leckie, "Representation of Mechanical Behavior in the Presence of Changing Internal Structure," *J. Applied Mech.*, ASME, **55**, 1 (1988).

Ouchiyama, N., and T. Tanaka, "Kinetic Analysis of Continuous Pan Granulation. Possible Explanations for Conflicting Experiments and Several Indications for Practice," *Ind. Eng. Chem. Process Des. Dev.*, **20**, 340 (1981).

Reyes, S. C., and E. Iglesia, "Monte Carlo Simulations of Structural Properties of Packed Beds," *Chem. Eng. Sci.*, **46**(4), 1089 (1991).

Rosen, J. M., "A Statistical Description of Coagulation," *J. Coll. Interface Sci.*, **99**(1), 9 (1984).

Rosner, D. E., A. G. Konstandopoulos, M. Tassopoulos, and D. W. Mackowski, "Deposition Dynamics of Combustion Generated Particles: Summary of Recent Studies of Particle Transport Mechanisms, Capture Rates and Resulting Deposit Microstructure/Properties," presented at the Engineering Foundation Conference: *Inorganic Transformations and Ash Deposition during Combustion*, March 10-15, 1991, Palm Coast, FL, in press (1991).

Satake, M., "Graph-Theoretical Approach to the Mechanics of Granular Materials," in *5th International Symposium on Continuum Models of Discrete Systems*, Nottingham, July 14-20, 1985, 163 (1985).

Schwartz, L. M., and J. R. Banavar, "Transport Properties of Disordered Continuum Systems," *Phys. Rev.*, **B 39**, 11965 (1989).

Scott, G. D., "Packing of Spheres," *Nature*, **188**, 908 (1960).

Seibert, D., "Darstellung interner Werkstoffstrukturen und Texturen," unpublished (1988).

Tassopoulos, M., *Relationships Between Particle Deposition Mechanism, Deposit Microstructure and Effective Transport Properties*, PhD Thesis, Yale University (1991).

Tassopoulos, M., and D. E. Rosner, "Simulation of Vapor Diffusion in Anisotropic Particulate Deposits," *Chem. Eng. Sci.*, in press (1991a).

Tassopoulos, M., and D. E. Rosner, "Effective Thermal Conductivity of Anisotropic Particulate Deposits," AIChE Meeting, paper 151d, Los Angeles (Nov. 17-22, 1991); submitted to *Int. J. Heat Mass Transfer*.

Thornton, C., and D. J. Barnes, "Computer Simulated Deformation of Compact Granular Assemblies," *Acta Mech.*, **64**, 45 (1986).

Torquato, S., "Thermal Conductivity of Disordered Heterogeneous Media from the Microstructure," *Rev. Chem. Eng.*, **4**, 151 (1987).
Torquato, S., "Random Heterogeneous Media: Microstructure and Improved Bounds on Effective Properties," *Appl. Mech. Rev.*, **44**(2), 37 (1991).
Tory, E. M., B. H. Church, M. K. Tam, and M. Ratner, "Simulated Random Packings of Equal Spheres," *Can. J. Chem. Eng.*, **51**, 484 (1973).
Tory, E. M., N. A. Cohrane, and S. R. Waddell, "Anisotropy in Simulated Random Packing of Equal Spheres," *Nature*, **220**, 1023 (1968).
Vicsek, T., *Fractal Growth Phenomena*, World Scientific, Teaneck, NJ (1989).
Visscher, W. M., and Bolsterli, "Random Packing of Equal and Unequal Spheres in Two and Three Dimensions," *Nature*, **239**, 504 (1972).
Zallen, R., "Stochastic Geometry: Aspects of Amorphous Solids," in *Fluctuation Phenomena*, Montroll, E. W., and J. L. Lebowitz, eds., North Holland, Pub. (1979).

Manuscript received July 10, 1991, and revision received Oct. 11, 1991.